Nat. Hazards Earth Syst. Sci., 10, 1269–1280, 2010
www.nat-hazards-earth-syst-sci.net/10/1269/2010/
doi:10.5194/nhess-10-1269-2010

Natural Hazards and Earth System Sciences

Numerical earthquake response analysis of the Liyutan earth dam in Taiwan

Z. Feng[1], **P. H. Tsai**[2], **and J. N. Li**[3]

[1]Department of Soil and Water Conservation, National Chung Hsing University, Taichung 402, Taiwan
[2]Department of Construction Engineering, Chaoyang University of Technology, Taichung, Taiwan
[3]Kingfeng County Government, Taitung, Taiwan

Received: 30 March 2010 – Revised: 21 May 2010 – Accepted: 27 May 2010 – Published: 17 June 2010

Abstract. The dynamic response of the Liyutan earth dam to the 1999 Chi-Chi earthquake (M_L=7.3) in Taiwan was numerically analyzed. First, the staged construction of the dam was simulated. Then, seepage analysis, considering a 60-m water level, was performed. After seepage analysis, the initial static stress (prior to dynamic loading) was established in the dam. Both the horizontal and vertical acceleration time histories recorded at the base of the dam were used in the numerical simulations. The dynamic responses of the dam were analyzed for 50 s in the time domain. The simulated results were in agreement with the monitored data. The transfer function analysis and Hilbert-Huang Transform (HHT) were used to compare the results and to perceive the response characteristics of the dam. In particular, the time-frequency-energy plots of the HHT can reveal the timing and time frame of the dominant frequencies of the dynamic response. The influences of the initial shear modulus and uni-axial earthquake loading were also investigated.

1 Introduction

The 21 September 1999 Chi-Chi earthquake (M_L=7.3) induced by the Chelunpu fault fracture caused very strong shaking in central Taiwan. The Liyutan earth dam experienced the earthquake and showed damage and deformation. A crack near the left abutment of the dam was observed. An inspection pit was excavated to a depth of approximately 2.5 m for examination. Based on the examination, the damage seemed to be manageable and minor. Strong motion records of the earth dam were captured during the earthquake. This dam is the closest earth dam to the Chelunpu thrust fault in Taiwan that has complete strong motion records (Fig. 1). Therefore, this dam presents a rare opportunity to simulate the strong earthquake response of an earth dam using a complete set of recorded data for comparison.

The earthquake performance of an earth dam is a very important safety issue. Seismic response evaluations of every earth dam in Taiwan are carried out at regular 5-year intervals. Recently, various approaches to the dynamic response analysis of earth dams have been applied. Cascone and Rampello (2003) used the equivalent linear method to account for non-linear soil behavior for the two-dimensional finite element (FE) dynamic analyses of an earth dam. They accounted for synthetic and real acceleration histories as the input motions. Rampello et al. (2009) analyzed the dynamic response for the same dam using the finite element method with a hardening soil model, and they back-analyzed the earth dam construction. Psarropoulos and Tsompanakis (2008) evaluated a tailing dam using a FEM code, PLAXIS, to study static and seismic loading. Parish et al. (2009) used a finite difference code, FLAC3D, to evaluate the seismic response of a 3-D earth dam for elastic and plastic responses by comparing velocity spectra. However, the input seismic velocity history at the foundation base was only uniaxial in the horizontal direction, and therefore, their analysis is still a 2-D model. In addition, the shear modulus and elastic modulus did not change with effective confining stress and remained constant throughout the analyses. Siyahi and Arslan (2008a, b) adopted a finite element framework, OpenSees, with pressure-dependent multi-yield materials to investigate the dynamic behavior, failure modes and mechanisms of failure of a dam. Hwang et al. (2007) studied the 42 earthquake records of the Liyutan earth dam and suggested the shear modulus of the dam. Their suggested shear

Correspondence to: Z. Feng
(tonyfeng@nchu.edu.tw)

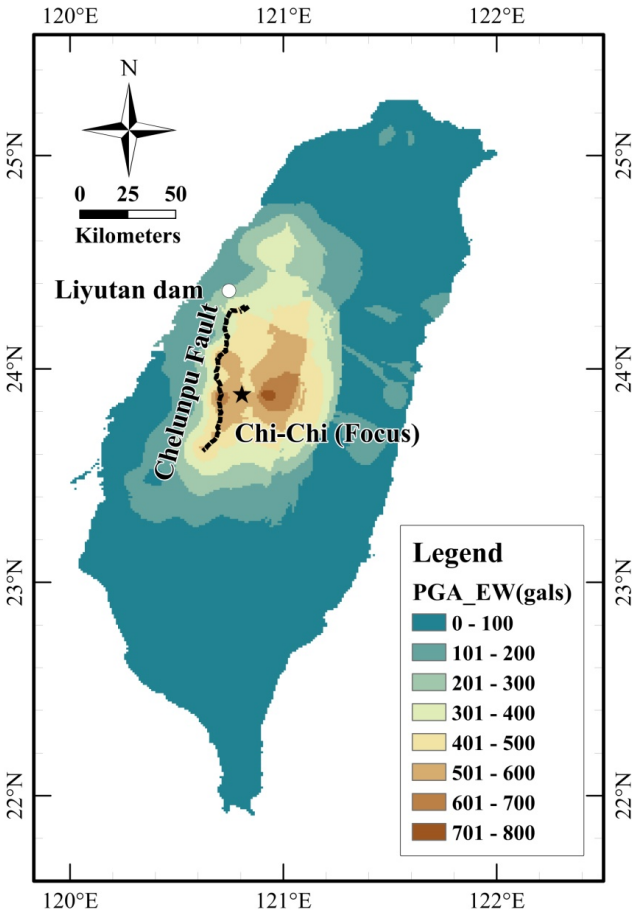

Fig. 1. Location of the Liyutan earth dam and distribution of East-West peak ground acceleration (PGA) during the 1999 Chi-Chi earthquake. (Note: the PGA data are after Central Weather Bureau Taiwan.)

modulus is referenced in this study for the purpose of comparison. Hwang et al. (2007) performed a frequency domain dynamic analysis using the FLUSH program (Lysmer et al., 1975) with an equivalent linear soil model for the dam for various peak ground accelerations (PGAs) up to 0.7 g. The studies mentioned above involved only uni-axial earthquake loading. Previously, we performed a preliminary dynamic response study of the Liyutan earth dam with bi-axial earthquake loading in the time domain (Feng et al., 2006); that dynamic response is investigated further and in more detail in this paper.

This study focuses on the dynamic response of the Liyutan earth dam during the 1999 Chi-Chi strong earthquake. Many of prior dynamic analyses were done in the frequency domain or with uni-axial loading. This study, however, performs time domain dynamic response analysis with bi-axial loading. Transfer function analysis and the Hilbert-Huang Transform (HHT; Huang et al., 1998) are adopted to present the differences between the simulated results of this study and the data from the monitored records. The HHT can clearly show the detailed dynamic responses of the dam in the frequency and time-frequency domains to compare and examine dynamic response characteristics. The analyzed results of the dam subjected to the Chi-Chi earthquake are validated by the monitored records. In addition to the validation, this study demonstrates that a higher initial shear modulus assignment to the dam produces a stronger response at high frequencies and predicts smaller deformation of the dam. The authors also prove with the analyzed results that bi-axial loading shows a stronger response, and thus, for dams close to a fault, the vertical earthquake loading should not be ignored. The simulation process of the Liyutan earth dam and interpretations of results presented in this study are straightforward and can be easily followed by researchers/engineers to perform dynamic earth dam analysis.

2 Site description and input motion

2.1 Description of the Liyutan earth dam

The Liyutan earth dam forms an off-channel reservoir located downstream of the Jing-Shan River in Miaoli, Taiwan. It is a roller-compacted earth dam measuring 96 m high and 235 m long with a top width of 10 m. A cross section of the dam, which illustrates its material composition, is shown in Fig. 2. Basically, the core is composed of impermeable material, and the shells are composed of semi-permeable material. The foundation materials are mostly sandstone, silt sandstone and shale, which are much stiffer than the dam materials and are not considered in the numerical model.

2.2 Material properties for numerical analysis

The material properties of the dam are simplified for numerical analysis in this study. The dam is divided into the upstream shell, downstream shell and the core. The core of the dam is mainly composed of impermeable clayey material and is classified as clay (CL), silty sand (SM), silt (ML) and clayey gravel (GC) by the Unified Soil Classification System. The shells are composed of excavated rocks and are semi-permeable. The filter, which is mainly present between the core and the downstream shell, is composed of gravel from the riverbed, and its properties are very close to those of the downstream shell. Therefore, for simplicity, the filter is merged into the downstream shell in the numerical model.

The initial shear modulus, G_{max}, in the numerical model was assigned according to shear seismic field test results, as shown in Fig. 3 (Central Water Resources Office, 1995), referring to the initial static stress state obtained previously. We also adopted the G_{max} suggested by Hwang et al. (2007) to compare the influence of the shear modulus of dam materials on the dynamic responses of the Liyutan earth dam.

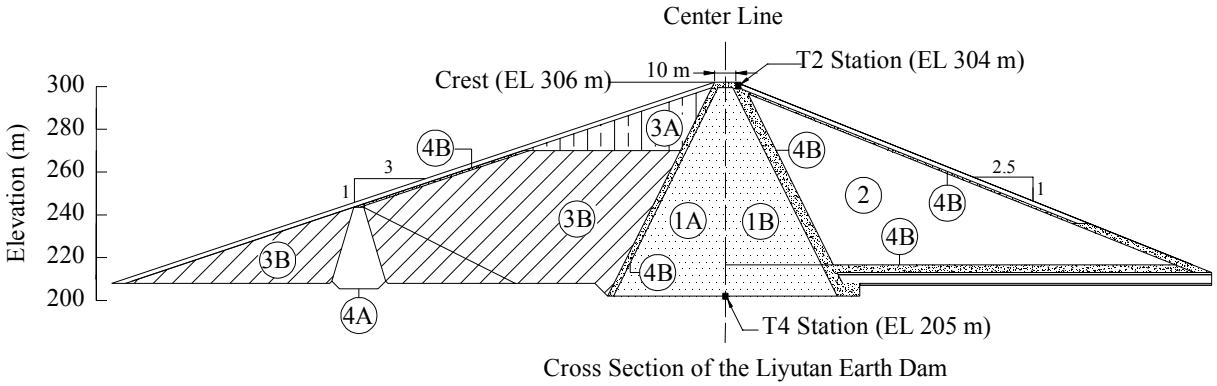

Fig. 2. Central cross-section and material zones of the Liyutan earth dam (re-plotted, Central Water Resources Office, 2000b).

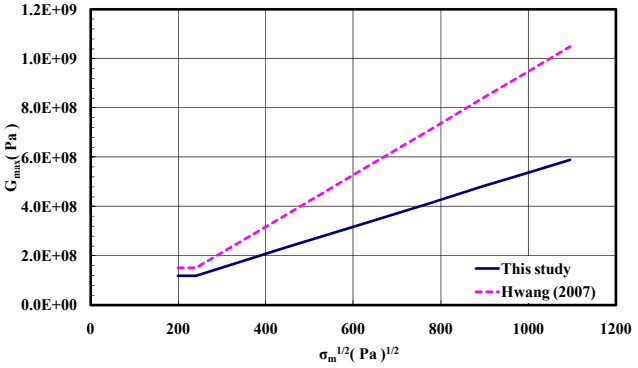

Fig. 3. Initial shear modulus, $G_{\max}$. The solid line indicates test results for the Liyutan earth dam (after Central Water Resources Office, 1995). The dashed line presents a synthetic trend, deduced from Hwang et al. (2007).

For the numerical analysis, the shells and core of the earth dam are assumed to satisfy the Mohr-Coulomb model. Field and laboratory tests were performed during and after construction by the Central Water Resources Office in Taiwan to evaluate the material properties of the dam. The evaluated properties for numerical simulations are listed in Table 1. Note that the shear modulus shown in Table 1 is only used to establish the initial static stress state during the simulation of dam construction. The initial shear modulus assigned in the dynamic analysis of each element will be re-calculated according to the mean effective stress and the curve presented in Fig. 3.

Table 1. Material parameters of the earth dam based on test data (Central Water Resources Office, 1995).

Zone	Shear modulus, G, Pa	Permeability, K, cm/s	Poisson's Ratio, υ	c', kPa	ϕ', deg
Upstream shell	5.0E8	5E-6	0.34	94	41
Core	3.5E8	1E-7	0.45	34	27
Downstream shell	6.0E8	5E-6	0.3	82	35

2.3 Shear modulus degradation and damping

The four-parameter sigmoidal (Sig4) model (Itasca, 2008) is adopted to fit the S-shaped shear modulus degradation curves of the shell and core materials. The model has proper asymptotic behavior. The equation of secant modulus, M_s, for the Sig4 model is

$$M_s = y_0 + \frac{a}{1+\exp(-(L-x_0)/b)} \quad (1)$$

where L is the logarithmic strain, $L = \log_{10}(\gamma)$, and γ is the cyclic strain. The values a, b, x_0 and y_0 are the four model parameters. The four parameters can be curve fitted by trial-and-error in a spreadsheet to resemble the normalized shear modulus reduction curves from material test results.

This study adopted the normalized shear modulus reduction curves obtained from the test results of the dam materials (Central Water Resources Office in Taiwan, 1995). The normalized shear modulus reduction ($G/G_{\max}$) versus shear strain curves with the fittings of the Sig4 model are demonstrated in Fig. 4. The fitted parameters of the sigmoidal model are listed in Table 2.

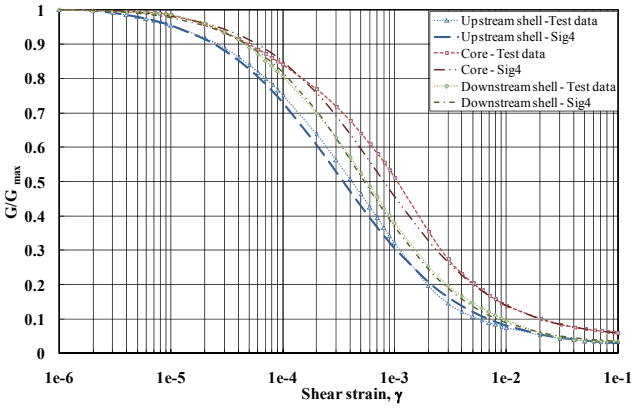

Fig. 4. Shear modulus reduction curves fitted by the Sig4 model for each zone.

Table 2. Parameters of the sigmoidal (Sig4) model for the shells and core.

Zone	a	b	x_0	y_0
Upstream shell	0.995	–0.55	–1.5	0.02
Core	0.963	–0.52	–1.15	0.045
Downstream shell	0.9789	–0.485	–1.3	0.027

The material damping ratios of the Liyutan earth dam obtained from the test results show that damping ratios are high even at a low cyclic strain level of 1×10^{-6}. Furthermore, the sigmoidal model dissipates almost no energy at a low cyclic shear strain level (Itasca, 2008). Additionally, when the Mohr-Coulomb material yields and undergoes plastic flow, both the 5% Rayleigh damping and the sigmoidal model will be "switched off" (Itasca, 2008). Therefore, to account for the high damping of the dam materials at low strain level, an additional 5% Rayleigh damping has been added in the dynamic analysis.

2.4 Input motion

The Chi-Chi earthquake acceleration time histories recorded at the T4 station at the base and central sections of the Liyutan earth dam were selected as the input motion for this study. The horizontal and vertical monitored acceleration time histories of the Chi-Chi earthquake were simultaneously considered as the bi-axial input to the base of the dam for a duration of 45 s in the dynamic analyses. The horizontal acceleration component is perpendicular to the longitudinal axis of the dam. In the Chi-Chi earthquake, the horizontal and vertical peak accelerations monitored at the base of the dam were 0.149 g and 0.108 g, respectively.

The displacement of the earth at the base should be zero after the earthquake, at which time the authors assume no permanent ground movement occurs. However, double integration of an acceleration record may not be zero due to noise or the threshold of the seismic instrument. Therefore, a baseline correction is applied for the two input acceleration time histories. The vertical and horizontal baseline-corrected acceleration time histories are shown in Fig. 5 with their respective Fourier spectra. The dominant frequencies of horizontal acceleration were approximately 0.244, 0.69, and 0.87 Hz. For vertical acceleration, the dominant frequency was approximately 0.255 Hz.

3 Analysis methods

The Fast Lagrangian Analysis of Continua (FLAC) 6.0 code (Itasca, 2008) is adopted in this study. The mid-section of the Liyutan earth dam was modeled as a 2-D grid. There are 1101 elements in the mesh, as shown in Fig. 6. Both the horizontal and vertical acceleration of the earthquake were applied to the dam. The acceleration and displacement time histories and permanent displacement of the dam can be obtained from the numerical results. The results were compared to the field measurement and to the acceleration histories recorded at the T2 station at the top of the dam.

3.1 Static analysis

To establish a reasonable stress state for the dam before dynamic analysis, the initial static equilibrium stress state was obtained. The staged construction was simulated by sequentially adding 20 layers of dam construction materials before water impounding. When a layer was added, a new static equilibrium for that stage of the dam construction was computed. This process was repeated until the full dam structure was formed. After the stage construction analysis, the displacements at each node of the mesh were reset to zero. The retaining water level of the Liyutan earth dam was 60 m when the Chi-Chi earthquake struck. Therefore, the steady state seepage analysis of the dam for a 60-m water level was performed. The seepage analysis was uncoupled from the mechanical analysis. The initial static stress state (prior to the earthquake) was then computed. The dam showed a slight movement to the upstream direction due to buoyancy forces in the upstream shell. The stress state at this stage is the initial stress condition of the dam before dynamic loading.

These static analyses yielded the following results: 1) the stress distribution after dam construction, 2) the pore water pressure distribution for steady state seepage, and 3) the initial stress state prior to the earthquake.

3.2 Dynamic analysis

By using the initial stress state obtained in the previous static analysis, the dam was modeled using the Chi-Chi earthquake bi-axial acceleration time history as a dynamic forcing term. The horizontal and vertical acceleration time-history recorded at the base of the dam are input simultaneously. The

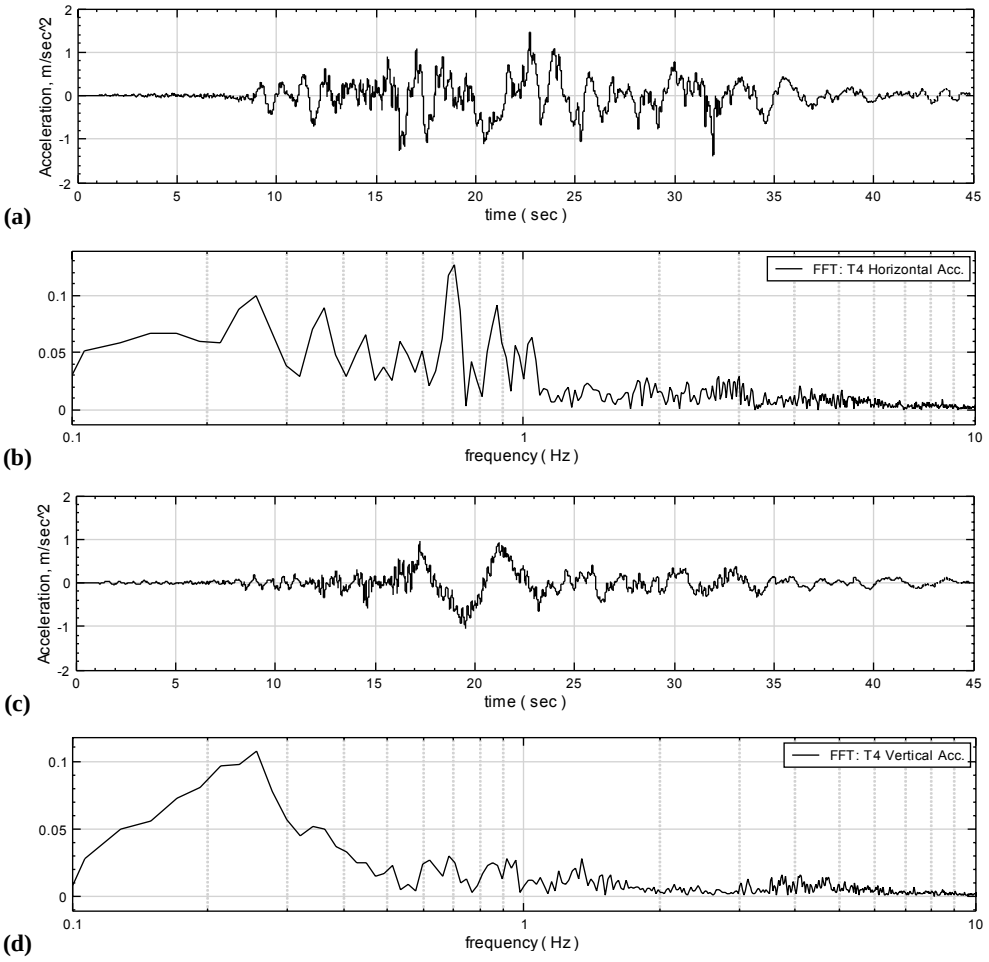

Fig. 5. (a) The recorded horizontal acceleration time history for the Chi-Chi earthquake at the T4 station at the base of the Liyutan dam. **(b)** Fourier spectra of the recorded horizontal acceleration of the earthquake at the T4 station. **(c)** The recorded vertical acceleration time history for the Chi-Chi earthquake at the T4 station at the base of the Liyutan dam. **(d)** Fourier spectra of the recorded vertical acceleration of the earthquake at the T4 station.

duration of the dynamic analysis is 50 s, which is five seconds more than the recorded input acceleration (45 s). The additional 5 s allows for attenuation of the transient response of the dam to the earthquake vibration.

3.3 Transfer function and Hilbert-Huang Transform

Transfer function analysis is employed in this study to compare the dynamic response of the dam in the frequency domain. Following Hwang et al. (2007), the transfer function is defined as the ratio of the Fourier amplitude response spectrum (RFRS) of the acceleration history of the crest divided by that of the base. The recorded acceleration at the base is defined as the input, and the acceleration response at the crest is the output.

For the time-frequency domain, the HHT is applied to obtain the acceleration time-frequency-energy spectra for comparison. HHT is a powerful method because of its adaptive and time efficiency. It is very good for analyzing nonlinear and non-stationary signals. Signals are first decomposed into intrinsic mode functions (IMFs) by the empirical mode decomposition method. The IMFs are then transformed using the Hilbert transform to obtain their instantaneous frequencies as a function of time. For details of the HHT method, readers should refer to Huang et al. (1998). The timing and time frame of the dominant frequencies of the dynamic response of a dam can be clearly revealed by HHT.

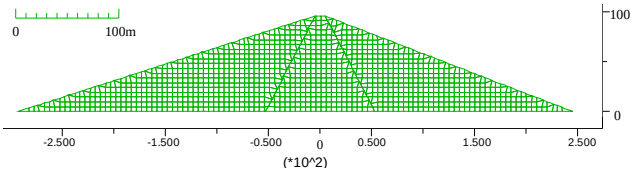

Fig. 6. The mesh for numerical analyses of the Liyutan earth dam.

Table 3. Comparisons of the calculated permanent displacements at the surface of the dam with the measured data (unit: cm).

	Upstream shell (mid-height) Horiz.	Upstream shell (mid-height) Vert.	Top of crest Horiz.	Top of crest Vert.	Downstream shell (mid-height) Horiz.	Downstream shell (mid-height) Vert.
Measured displacement[1]	–2.7∼–3.9	–5.4∼–6.8	–0.7∼–4.3	–5.0∼–7.9	1.8∼2.9	–2.6∼–3.4
Calculated displacement	–2.0	1.3	–5.5	–5.8	–0.4	0.2

[1] Survey results after the Chi-Chi earthquake from the Central Water Resources Office (1999).
[2] Negative signs (–) represent horizontal leftward displacement or vertical downward displacement.

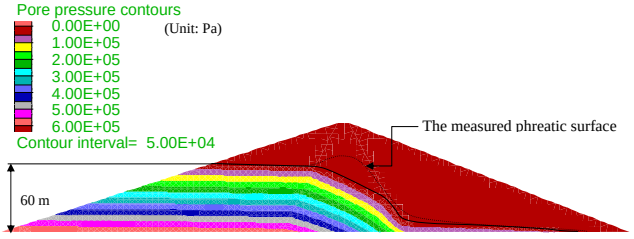

Fig. 7. The pore pressure distribution derived from the seepage analysis. The dotted line shows the in-situ measured phreatic surface. Height of retained water is 60 m.

4 Results and discussion

4.1 Seepage analysis

The result of the steady state seepage calculation is shown in Fig. 7. The largest static pore water pressure was found to be 600 kPa. The phreatic surface depresses quickly in the downstream shell. Overall, the trends of the calculated phreatic surface are reasonable and close to field measurement data (Central Water Resources Office, 2000a) with the exception of those in the core zone. The field measurement of the phreatic surface in the core zone is higher because the seepage remains in a transient state, as opposed to steady state. In addition, the materials in the core zone are relatively impermeable, whereas the shell materials are semi-permeable. Therefore, the lowering of the phreatic surface in the core zone occurs more slowly than in the shells. This study considers only steady state seepage, which may overestimate the effective stress distribution in the core zone and slightly overestimate the G_{max} in the core zone. Further study on transient seepage in the core zone may improve the accuracy of the estimations.

4.2 Deformation of the dam

The exaggeratedly deformed mesh (after the 50-s earthquake) is shown in Fig. 8. The displacements are the permanent deformation after the earthquake simulation. The dam mostly deformed toward the upstream side with a maximum displacement of 8.7 cm. A potential sliding surface is located at two-thirds of the height of the dam in the upstream shell. The upstream shell is mostly submerged under water, and its shear strength is smaller due to a lower effective stress. Overall, the calculated displacements are fairly close to the field-measured data (Table 3). The simulated displacement at the dam crest was the best fit with the field data; however, larger discrepancies appear at the mid-height of the upstream and downstream shells. These discrepancies could be caused by use of the triangular mesh for the dam, which is fixed at the base and thus constrains the deformability of the dam and prevents sliding at the base of the dam. Relative horizontal and vertical displacement differences between the top and base of the dam during the earthquake simulation are depicted in Fig. 9. The maximum relative horizontal displacement is 14.9 cm toward upstream. The permanent horizontal displacement is 5.5 cm. The maximum relative vertical displacement is 6.2 cm downward, and the permanent vertical displacement is 5.8 cm.

4.3 Distribution of the maximum acceleration of each element

The maximum accelerations of each element during the 50 s of earthquake simulation were calculated. The distributions of the maximum horizontal and vertical accelerations are depicted in Fig. 10a and b. For horizontal movement, higher accelerations are mainly located at the top portion of the dam. For vertical movement, higher accelerations are located at the mid-height of the upstream and downstream shells. Apparently, horizontal accelerations are generally larger than vertical acceleration for most elements.

4.4 Acceleration response at the crest

The calculated acceleration time histories at the crest of the dam and its RFRS and HHT spectra are discussed. Corresponding plots of the recorded data are presented for comparison in Figs. 11–14. The computed horizontal and vertical peak accelerations are 0.269 g and 0.133 g, which are close to the recorded peak accelerations of 0.24 g and 0.15 g,

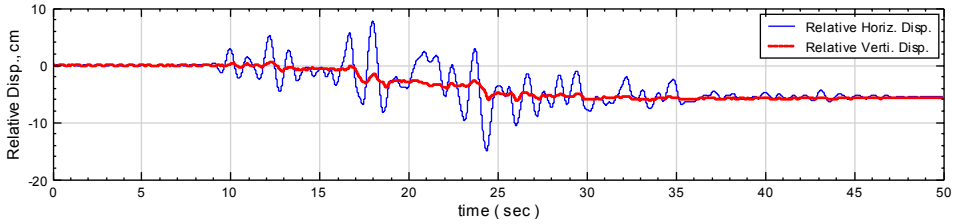

Fig. 8. Exaggerated grid distortion after shaking. Maximum displacement = 8.7 cm; displacement magnification = 100 times. The dotted line represents the sliding surface of the displaced block. The movement is toward the upstream side of the dam.

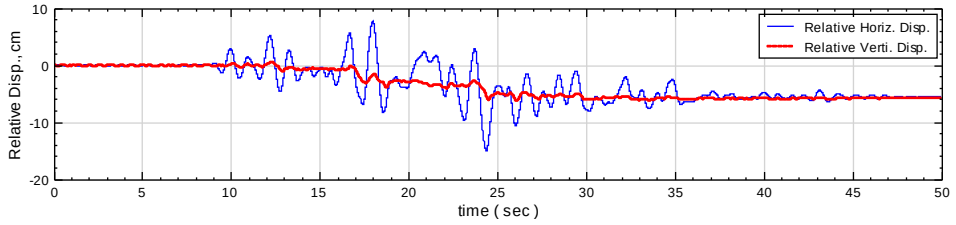

Fig. 9. Relative horizontal and vertical displacements between the crest and base of the dam.

respectively; refer to Figs. 11a, b and 12a, b. For horizontal vibration, the transfer functions (RFRS) versus frequency are shown in Fig. 11c for the calculated results and Fig. 11d for the recorded data. The frequencies of the "peaks" in RFRS are similar to those shown in Fig. 11c and d. When the frequency is lower than 5 Hz, the two RFRS fit well. When the frequency is greater than 5 Hz, the RFRS of the recorded data are generally larger than those of the calculated result. The amplification of the high frequency region is not obvious in the numerical calculation, which may be due to limitation of the element size. Similar results are observed for vertical vibration, as shown in Fig. 12c and d. The RFRS of the calculated result are smaller than the RFRS of the recorded data when the frequency is greater than 5 Hz.

The time-frequency-energy spectra of the Hilbert-Huang Transform of the accelerations at the dam crest can be evaluated from Figs. 13 and 14. In these figures, higher energy instantaneous frequencies are shown in dark red, and lower energy frequencies are presented in a lighter color. The HHT spectra of the calculated results and recorded data at the T2 station are qualitatively similar. For the horizontal vibration at the dam crest, the dominant frequencies with higher energy are approximately 0.6∼1.2 Hz and vary with time (Fig. 13). At 0.244 Hz and 0.69 Hz, the dominant frequency of the input horizontal acceleration at the base shows high energy (Fig. 13a and b). Energy above 3 Hz is insignificant, as shown in Fig. 13. For vertical vibration at the crest (Fig. 14), the energy is much lower than the energy of the horizontal shaking. The input vertical acceleration at the base, with a dominant frequency of 0.255 Hz, controls the response. Vertical vibration energy near this frequency is stronger along the time axis from 15 to 25 s (Fig. 14).

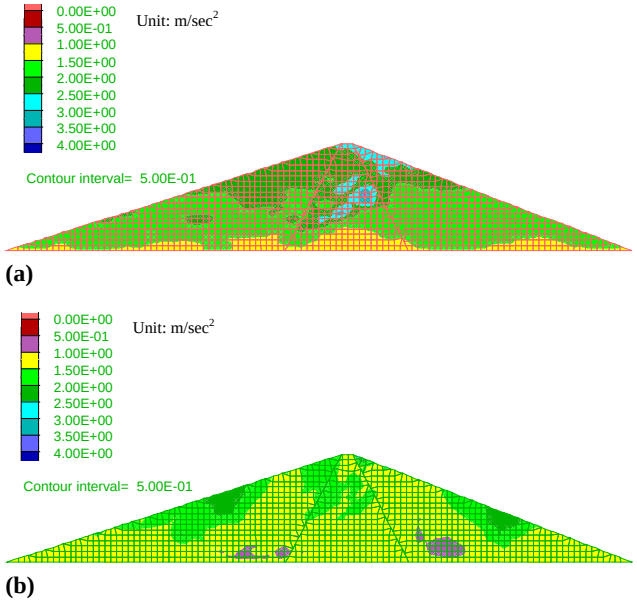

Fig. 10. **(a)** The maximum horizontal acceleration distribution of the dam during the 45 s of earthquake simulation. **(b)** The maximum vertical acceleration distribution of the dam during the 45 s of earthquake simulation.

4.5 Influence of G_{max}

This study assigns the initial shear modulus, G_{max}, of the dam materials according to field and laboratory test results from the Central Water Resources Office. The initial shear modulus is assigned to each element according to the effective mean stress of that element. Hwang et al. (2007) recommended a higher initial shear modulus of the dam (Fig. 3),

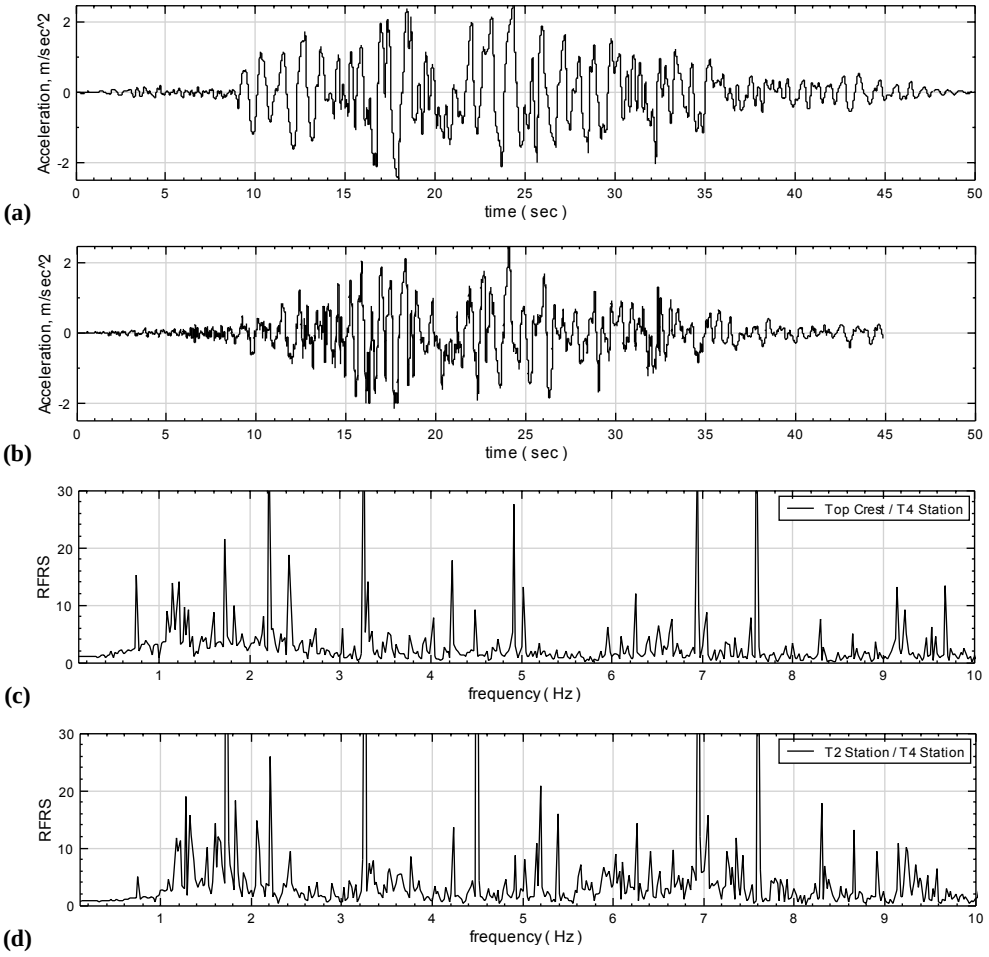

Fig. 11. Comparison of the horizontal acceleration response at the crest and recorded T2 station. **(a)** Calculated horizontal acceleration at the crest. **(b)** Recorded T2 horizontal acceleration at the crest. **(c)** Transfer function (RFRS) between the horizontal response of the calculated result and the recorded T4 station. **(d)** Transfer function (RFRS) between the recorded horizontal response at the T2 and T4 stations.

and this suggestion is used to evaluate the influence of $G_{\max}$ on the dynamic response of the dam in this study. The transfer functions (RFRS) obtained from the data recorded at the T2 and T4 stations are compared in Fig. 15. For the RFRS of horizontal acceleration (Fig. 15a), this study fits the recorded RFRS better in the 1.1∼1.5 Hz band than the results obtained using the $G_{\max}$ from Hwang et al. (2007). This frequency range is near the fundamental frequency of the dam during the Chi-Chi earthquake. The horizontal fundamental frequency of the dam during the Chi-Chi earthquake is approximately 1.30 Hz, as suggested by Hwang et al. (2007). For 0.5∼1.0 Hz, the RFRS results obtained using the $G_{\max}$ from Hwang et al. (2007) match the recorded RFRS better than the RFRS obtained using the $G_{\max}$ estimated in this study. At a higher frequency range, 2.5∼3 Hz, the RFRS results obtained using the $G_{\max}$ suggested by Hwang et al. (2007) show a stronger response than those using the $G_{\max}$ estimated in this study. It is possibly due to the high initial shear modulus assignment. The same phenomenon is observed in Fig. 15b for the RFRS of the vertical response in the frequency range 2.6∼3 Hz. For the vertical response, the vertical fundamental frequency of the dam during the Chi-Chi earthquake is approximately 2.04 Hz, as indicated by Hwang et al. (2007), while the vertical fundamental frequency is near 1.95∼2 Hz based upon the RFRS of the recorded data presented in Fig. 15b. The RFRS results obtained using the two $G_{\max}$ assignments match the recorded RFRS quite well for low frequencies below 1.9 Hz. For the displacement aspect, the maximum permanent displacement found in this study is 8.7 cm, while the maximum permanent displacement obtained using the higher initial shear moduli according to Hwang et al. (2007) is only 2.9 cm. This value is much smaller than that found in the field survey data, as indicated in Table 3.

Therefore, assigning a higher initial shear modulus to the dam materials could cause a stronger response in the higher frequency range, which will predict less deformation of the dam.

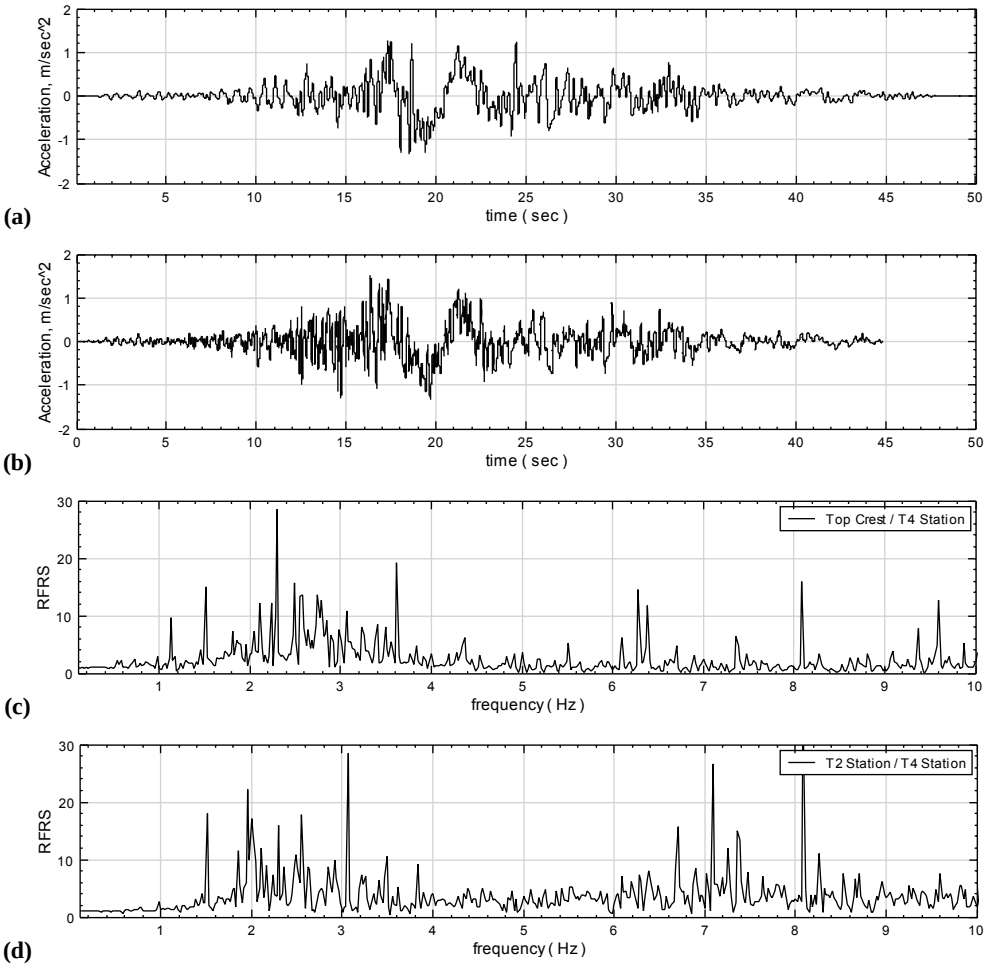

Fig. 12. Comparison of the vertical acceleration response at the crest and recorded T2 station. **(a)** Calculated vertical acceleration at the crest. **(b)** Recorded T2 vertical acceleration at crest. **(c)** Transfer function (RFRS) between the vertical response of the calculated result and the recorded T4 station. **(d)** Transfer function (RFRS) between the recorded vertical response at the T2 and T4 stations.

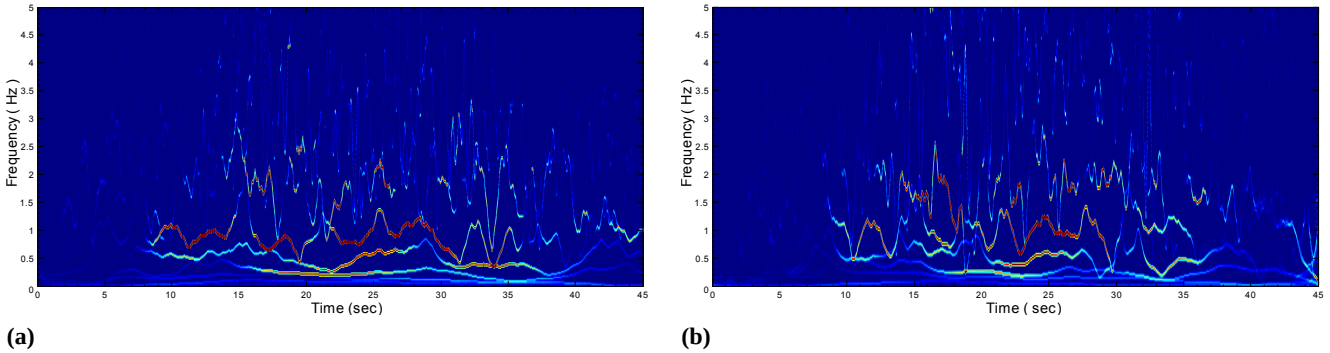

Fig. 13. Comparison of the HHT time-frequency spectra for the calculated horizontal acceleration at the crest and that of the recorded T2 station. **(a)** HHT time-frequency-energy spectra for the calculated horizontal acceleration at the crest. **(b)** HHT time-frequency-energy spectra for the horizontal acceleration of the T2 station at the crest.

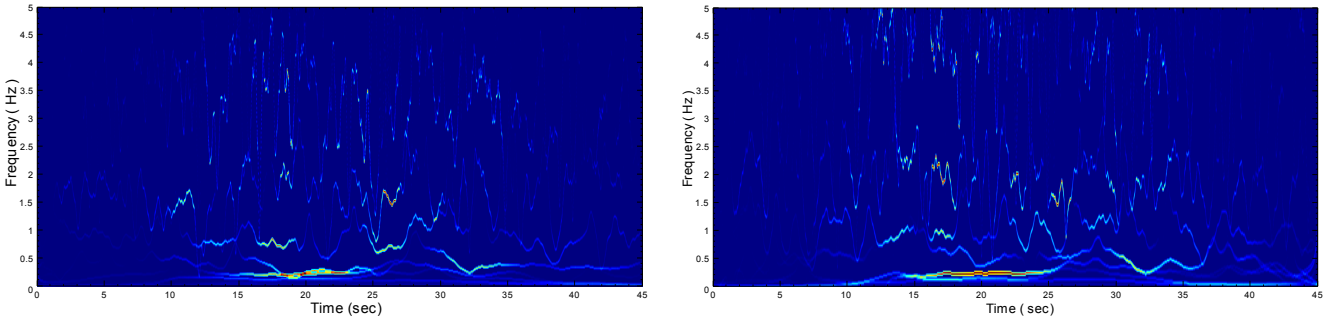

(a) **(b)**

Fig. 14. Comparison of HHT time-frequency spectra for the calculated vertical acceleration at the crest and that of the recorded T2 station. **(a)** HHT time-frequency-energy spectra for the calculated vertical acceleration at the crest. **(b)** HHT time-frequency-energy spectra for the vertical acceleration of the T2 station at the crest.

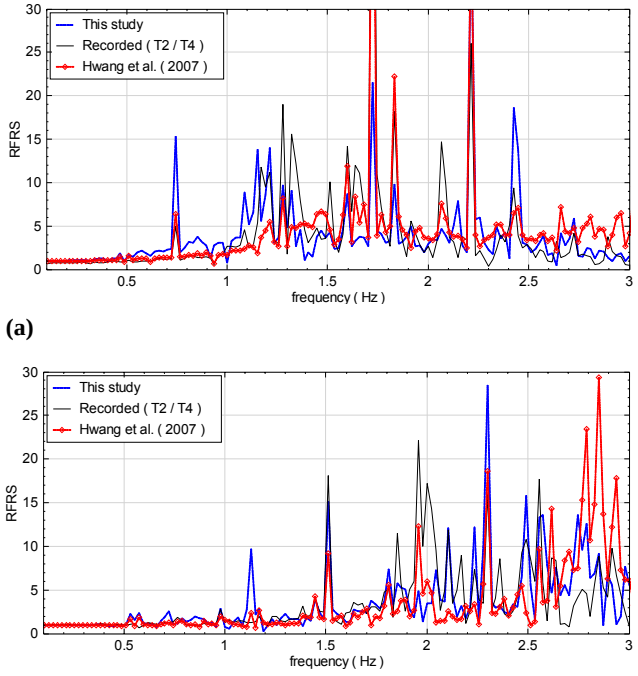

(a)

(b)

Fig. 15. Comparison of transfer function (RFRS) to illustrate the influence of G_{max} assignment. **(a)** Comparison of transfer function (RFRS) for horizontal acceleration. **(b)** Comparison of transfer function (RFRS) for vertical acceleration.

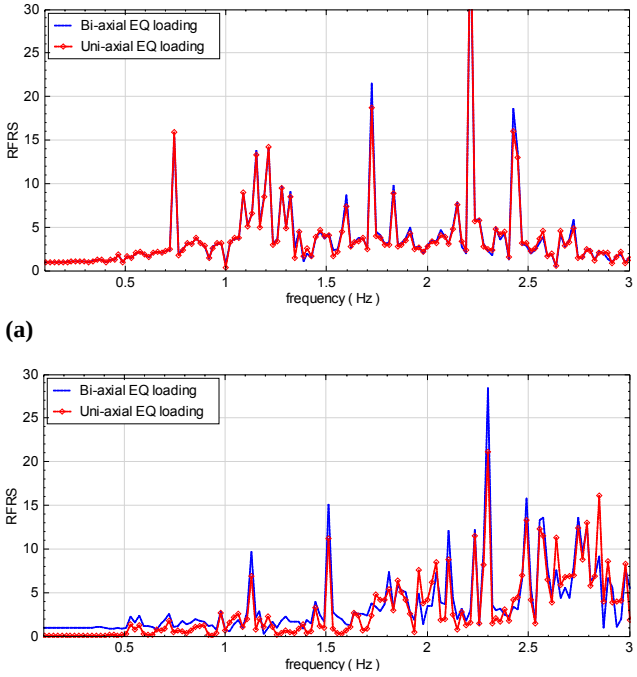

(a)

(b)

Fig. 16. Comparison of responses between bi-axial and uni-axial EQ loading. **(a)** Comparison of transfer function (RFRS) between bi-axial and uni-axial EQ loading for horizontal acceleration. **(b)** Comparison of transfer function (RFRS) between bi-axial and uni-axial EQ loading for vertical acceleration.

4.6 Influence of uni-axial and bi-axial earthquake loading

A simulation that only accounted for horizontal acceleration as the input earthquake loading was performed as a uni-axial case to evaluate the difference in response between uni-axial and bi-axial earthquake loading. The transfer functions (RFRS) of the horizontal acceleration between the two cases are almost identical (Fig. 16a); however, the bi-axial case showed a stronger response. For vertical acceleration, large differences are obvious when the frequency is smaller than 1.5 Hz (Fig. 16). For frequencies higher than 1.5 Hz, the RFRS between the two cases are fairly close because the vertical acceleration response of the dam crest in uni-axial loading is caused by the reflection of waves in the dam body

generated by horizontal vibration. The permanent displacement of the uni-axial loading case is 7.0 cm, which is 1.7 cm smaller than that of the bi-axial loading case.

In this study, the vertical acceleration of the Chi-Chi earthquake is not obvious because the vertical PGA is only 0.108 g; therefore, the horizontal responses of the uni-axial and biaxial loading cases are very similar. If only the horizontal vibration component of the dam is required, the vertical acceleration input may be omitted. However, if a dam is close to a fault, the vertical shaking could be serious, and vertical acceleration should not be ignored.

5 Conclusions and suggestions

The aim of this study was to simulate the dynamic response of the Liyutan earth dam when it was struck by the 1999 Chi-Chi earthquake (M_L=7.3). The response of the dam was analyzed in the time domain using bi-axial earthquake loading. The results were presented for comparison in the form of the transfer functions (RFRS) and HHT. The influence of the initial shear modulus was investigated, and the response of the dam to uni-axial earthquake loading was compared.

The following conclusions can be drawn from this study:

1. The simulation process used in this study includes the dam construction phase, steady state seepage, initial static stress state and dynamic analysis. This simulation process is straightforward, and, when the results are compared with the recorded data, they are validated with satisfaction.

2. The steady state seepage analysis result represents the phreatic surface quite well, with the exception of the core zone. Thus, the effective stress and shear modulus may be slightly over-estimated in the core zone.

3. A potential sliding surface moving toward the upstream side was found, located at two-thirds of the height of the dam. The calculated displacements are fairly close to the field-measured data, and the permanent displacements at the dam crest fit well with the in-situ survey data. The maximum permanent displacement of the dam from the numerical simulation is 8.7 cm.

4. Higher horizontal accelerations are located at the top portion of the dam. However, higher vertical accelerations are located at the mid-height of the upstream and downstream shells, as indicated by the results of the analysis.

5. Based upon comparison of the transfer functions (RFRS), the simulated acceleration at the crest fit well when compared to the recorded data, with the exception of the high-frequency region. The HHT spectra can show which periods have high energy in the dominant frequencies during earthquake shaking. The transfer function analysis and Hilbert-Huang Transform provide tools to reveal the details of the response characteristics of the dam.

6. For the two initial shear modulus assignments, the transfer functions match the recorded ones fairly well, with the exception of some frequency ranges. Generally, a higher initial shear modulus assignment produces a stronger response at high frequencies and predicts smaller deformation of the dam.

7. The transfer functions (RFRS) of horizontal acceleration between the uni-axial and bi-axial loading are almost the same. However, the bi-axial case shows a stronger response. The vertical acceleration response of the crest in uni-axial loading is caused by the reflection of waves generated by the horizontal vibration and is present at frequencies higher than 1.5 Hz. Vertical acceleration loading should not be omitted in dynamic analysis for those dams subjected to high vertical shaking.

In this study, the equivalent linear sigmoidal model with the Mohr-Coulomb model was used. Therefore, the excess pore water pressure generated during the earthquake was not predicted. Further study of the earth dam can be focused on applying a nonlinear cyclic plasticity model for the dam materials, especially for the upstream shell, which has a higher liquefaction potential. In addition, further parametric study can be useful for detailed examination of the dynamic response of an earth dam. It can be considered by varying the retaining water level, buck modulus, shear modulus, material damping, input motion, and peak ground acceleration.

Acknowledgements. This study was funded by the National Science Foundation of Taiwan (NSC-93-2211-E-005-11-), and their support is highly appreciated. Also, the authors would like to acknowledge the Central Water Resources Office in Taiwan for providing the monitored data and reports of the Liyutan dam.

Edited by: M. E. Contadakis
Reviewed by: M. Sadek and H. Arslan

References

Cascone, E. and Rampello, S.: Decoupled seismic analysis of an earth dam, Soil Dyn. Earthq. Eng., 23, 349–365, 2003.

Central Water Resources Office: Regular monitoring and analysis report of Liyutan dam, Central Water Resources Office, Taichung, Taiwan, 1995 (in Chinese).

Central Water Resources Office: Chi-Chi earthquake analysis report of Liyutan dam, Central Water Resources Office, Taichung, Taiwan, 1999 (in Chinese).

Central Water Resources Office: Regular monitoring and analysis report of Liyutan dam, Central Water Resources Office, Taichung, Taiwan, 2000a (in Chinese).

Central Water Resources Office: Report on earthquake monitoring and equipment maintenance of Liyutan dam, Central Water Resources Office, Taichung, Taiwan, 2000b (in Chinese).

Feng, Z., Tsai, P. H., Chang, Y. H., and Li, J. N.: Dynamic response of Liyutan earthdam subjected to the 1999 Chi-Chi earthquake in Taiwan. FLAC and Numerical Modeling in Geomechanics-2006, in: Proceedings of the 4th International FLAC Symposium, Madrid, Spain, 29–31 May 2006.

Huang, N. E., Shen, Z., Long, S. R., Wu, M. C., et al.: The empirical mode decomposition and the Hilbert spectrum for nonlinear and non-stationary time series analysis, Proc. R. Soc. Lon. Ser.-A, 454, 903–995, 1998.

Hwang, J. H., Wu, C. P., and Wang, S. C.: Seismic record analysis of the Liyutan earth dam, Can. Geotech. J., 44, 1351–1377, 2007.

Itasca Consulting Group, Inc.: FLAC – Fast Lagrangian Analysis of Continua, Ver. 6.0 User's Manual, Itasca, Minneapolis, 2008.

Lysmer, J., Udaka, T., Tasi, C. F., and Seed, H. B.: A computer program for approximate 3-D analysis of soil-structure interaction problems, EERC 75-30, Earthquake Engineering Research Center, Berkeley, California, 1975.

Parish, Y., Sadek, M., and Shahrour, I.: Review Article: Numerical analysis of the seismic behaviour of earth dam, Nat. Hazards Earth Syst. Sci., 9, 451–458, doi:10.5194/nhess-9-451-2009, 2009.

Psarropoulos, P. N. and Tsompanakis, Y.: Stability of tailings dams under static and seismic loading, Can. Geotech. J., 45, 663–675, 2008.

Rampello, S., Cascone, E., and Grosso, N.: Evaluation of the seismic response of a homogeneous earth dam, Soil Dyn. Earthq. Eng., 29, 782–798, 2009.

Siyahi, B. and Arslan, H.: Earthquake induced deformation of earth dams, B. Eng. Geol. Environ., 67, 397–403, 2008a.

Siyahi, B. and Arslan, H.: Nonlinear dynamic finite element simulation of Alibey earth dam, Environ. Geol., 54, 77–85, 2008b.